Evaluation of a Drone and Laser-Based Methane Sensor for Detection of a Surface Release of Methane

submitted to

BC Oil and Gas Research and Innovation Society

by

Dwayne Tannant, Wenbo Zheng, Kalie Smith, Aaron Cahill

University of British Columbia

December 31, 2018

a place of mind
THE UNIVERSITY OF BRITISH COLUMBIA

BC OGRIS
BC Oil and Gas
Research and Innovation Society

Table of Contents

List of Figures

List of Tables

Executive Summary

Fieldwork was conducted in August 2018 as an extension to work performed the previous summer to evaluate the capabilities of a laser-based methane sensor mounted to a drone for detecting and measuring near-surface methane concentration. Surface and airborne tests were performed in an open field near Hudson Hope, B.C.

The fieldwork evaluated a Laser Methane mini-G (Blue-Tooth capable) methane sensor along with an Android smartphone running a GasViewer app to log the data. The methane sensor is normally used as a hand-held device to measure the average methane concentration in a column of air through which a laser beam from the sensor passes. Concentration measurements were obtained every 0.1 seconds.

The methane sensor was tested 1 m above the ground level by shooting the laser beam horizontally at reflective targets. The test results verified that the sensor functioned properly. The measured background or ambient methane concentration in the air ranges between 0.5 and 3 ppm, so this range was used as a basis to determine whether the sensor was measuring methane concentrations higher than background levels. When methane gas was released into the air at a release rate of 30 m^3/day, elevated methane concentrations were detected, especially downwind of the release point.

For the airborne tests, the methane sensor was mounted to shoot vertically downward beneath a DJI Spread Wings S1000 multirotor drone. The methane release rates for the airborne tests ranged from 10 to 30 m^3/day. The drone was flown at an altitude of 10 m above the ground. The flight durations were in the range of 2 to 5 minutes. Numerous difficulties were encountered during the flights associated with the drone battery and flight controller.

The maximum practical height for using a Laser Methane mini-G sensor when flying over grassy terrain or low vegetation is approximately 10 m above the ground. If flying over a well pad without vegetation, a slightly higher altitude would probably also work. The test flights detected elevated methane concentrations around a surface release point for methane. However, the flights did not enable mapping of a methane plume or large areas of elevated methane concentrations. Variations in the wind velocity and direction quickly dissipated the methane.

A large drone is needed to carry the Laser Methane mini-G, which greatly increases the complexity for conducting airborne measurements versus ground-based measurements. This creates the need for a highly trained crew to perform the field measurements. Until a lightweight version of a laser-based methane sensor is developed specifically for drone-based measurement applications, there are significant challenges to wider adoption of the existing technology for routine methane measurement in the oil and gas sector.

Acknowledgments

The BC Oil and Gas Research and Innovation Society (BC OGRIS) funded the research presented in this report. The project received guidance from Brian Thomson from BCOGRIS and feedback from an advisory committee consisting of Laurie Welch and Kevin Parsonage from BCOGC and Steven Rogak from UBC. Andy Black's research group at UBC provided the eddy covariance data. The laser-based methane sensor was provided by Hetek Solutions Inc. The image processing software was provided by Dwayne Tannant's research lab.

1 Introduction

Manually measuring methane concentration at the ground level to detect fugitive methane emissions is time-consuming, expensive, and potentially threatening to human health and safety. This study evaluated the use of a drone equipped with a methane sensor as a more efficient method for methane detection and monitoring. The first phase of the fieldwork was performed in August and September 2017 to evaluate the capabilities of a laser-based methane sensor mounted to a multirotor drone for this purpose. Flights were flown manually over a subsurface injection site located within a narrow corridor between trees, while other flights flew over an uncontrolled release of methane in an open field. Methane concentrations exceeding background levels were measured in both experiments.

The second phase of fieldwork was conducted in August 2018 to evaluate further the use of a multirotor drone equipped with a laser-based methane sensor for detecting and monitoring methane emissions. This report covers the results of the second phase of the work. The research is an extension of the experiment and results described in a report previously submitted to BC OGRIS on February 1, 2018, titled "Evaluation of a Drone and Laser-Based Methane Sensor for Detection of Fugitive Methane Emissions" (Tannant et al. 2018). For the 2018 experiments, the goal was to fly the drone in a grid pattern as well as to conduct ground-based measurements for comparison.

The fieldwork took advantage of a much larger study being conducted by the Energy and Environment Research Initiative (EERI) operated out of the Department of Earth, Ocean and Atmospheric Sciences at UBC Vancouver. For more information on EERI and the research project, see http://eeri.ubc.ca/. The fieldwork was able to take advantage of an existing test site near Hudson Hope B.C. including a metered release of compressed methane gas and nearby eddy covariance instrumentation for weather data.

2 Equipment and Software

2.1 Methane Sensor and Smartphone App

A Laser Methane mini-G (LMm-G) laser methane sensor provided by Hetek Solutions Inc. was used for the research. This device is typically used as a handheld sensor in the natural gas industry. More information and specifications about this particular sensor can be found in the previous report submitted to BC OGRIS in early 2018 (Tannant et al., 2018). The sensor measures methane concentration by shooting a laser beam through a column of air between the sensor and a reflective surface. The sensor records the methane concentration in ppm of methane multiplied by the distance between the sensor and a reflective surface.

The methane measurements were recorded using GasViewer, a software application for Android devices, developed by Tokyo Gas Engineering Co., Ltd. The sensor readings were transferred from the sensor using a standard Bluetooth link to an Android phone. The sensor

was set to measure methane concentrations at a rate of 10 Hz. For each reading that is taken, the concentration measurement in ppm·m, intensity measurement, and error code are recorded along with the time. In addition, the approximate coordinates are obtained from the phone's GPS and recorded every 0.5 seconds. The GasViewer app stores the data for each series of measurements in a separate CSV file. Information about the meaning of the intensity and error code readings can be found in the previous report (Tannant et al., 2018).

The methane sensor with mounting attachments and the smartphone used for data storage weighs approximately 1 kg.

The results of the field tests in 2017 suggested that the measuring distance from the methane sensor to a grassy surface should not exceed roughly 15 m to avoid excessive non-reliable measurements. Before the field tests this year, the Laser Methane mini-G was tested by shooting the laser beam to a variety of surface types at a range of distances. The results showed that the surface significantly influenced the intensity of the reflected beam recorded by the sensor. When shooting to a white glossy surface, it was found that the measuring distance can be as far as 30 m with reliable measurements. Therefore, for the 2018 experiments, the drone was flown at the height of 10 m. At this height, less than 13% of the obtained concentration data were found to have error codes that indicate non-reliable measurements.

2.2 Drone and Mounting Device

A DJI Spread Wings S1000 multirotor drone was used to carry the sensor payload for the airborne experiments. The drone was flown by Vector Geomatics Land Surveying Ltd. The drone can safely carry a 4.4 kg payload for 10 min with a single 6S 16000 mA LiPo battery module. Additional specifications of the drone, including its GPS and autopilot systems, can be found in the previous report (Tannant et al., 2018). The drone recorded its GPS location, altitude above takeoff, and time every 0.5 seconds during the flights. These data were later provided by Vector in a csv file.

A custom-designed aluminum mounting plate was made to hold the methane sensor in a vertically downward orientation and to hold the smartphone, such that the sensor was centred below the centre of the drone and did not hang below the drone's support legs. Details on this arrangement can also be found in the previous report (Tannant et al., 2018).

2.3 Equipment for Ground-Based Measurements

The methane sensor was attached to a customized frame that was bolted to a tribrach for a surveyor's tripod. The tribrach allowed the sensor to rotate about a vertical axis to shoot laser beams in different directions. A reflective target (a square black-painted wood plate with a white circular reflective glossy dot in the centre) was strapped to an adjustable surveying pole. Bubble levels on the survey tripod and the surveying pole were used for levelling purposes. Measurements of methane concentration were obtained by shooting laser beams horizontally from the survey tripod to the reflective target at a known distance.

3 Field Experiments

3.1 Locations

The field experiments were conducted in a large open, grassy field located northeast of Hudson Hope B.C. (Figure 1). The experiments were conducted on August 29 and 30, 2018. The testing took advantage of an available site and a supply of methane gas from a larger field experiment involving controlled subsurface injections of methane gas. The larger research project is examining the impacts of released natural gas and the migration patterns of the methane gas for different hydrogeological and atmospheric conditions. This research is being conducted as part of the Energy and Environment Research Initiative (EERI) being operated out of the Department of Earth, Ocean and Atmospheric Sciences at UBC Vancouver (Cahill et al. 2018).

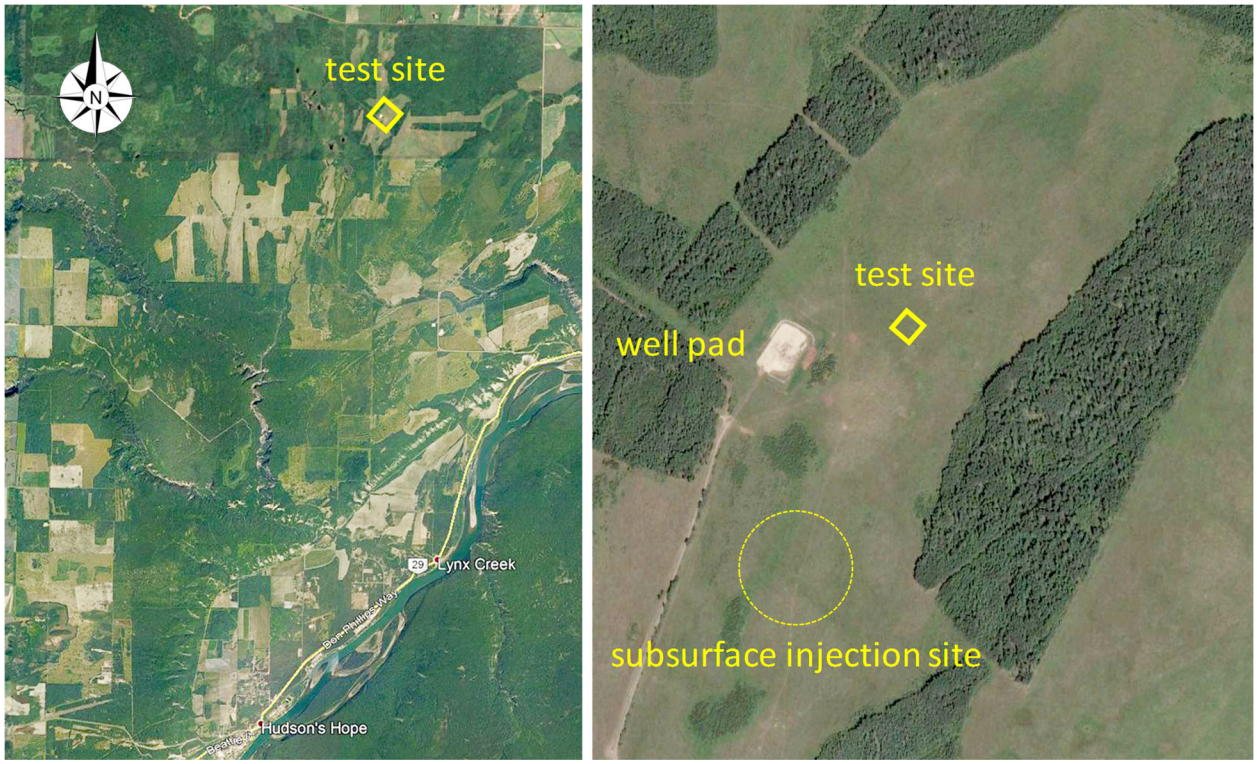

Figure 1. Location of the open field used for the field experiments (images from GoogleEarth).

Controlled surface releases from a tank of methane gas occurred on August 29 for the ground-level measurements and on August 30 for the drone flights. There is also an abandoned well pad nearby. Hand-held methane measurements were taken by walking around the subsurface injection site, and the abandoned well pad found that the methane concentrations were less than the background levels (<3 ppm). Thus, no flights were flown over the subsurface injection site or the abandoned well pad. The open field is northeast of the subsurface injection site and the abandoned well pad.

An orthophotograph of the open field constructed from a series of aerial photographs taken on August 30 by a drone is shown in Figure 2. The methane release point was set up on a cattle trail in the open field. A gas line from a tank of compressed natural gas was attached to a wooden stake driven into the ground in the centre of the test area (red circle). The test location covered a square 40 m by 40 m area defined by four blue 20 l pails placed on the ground. The four corners of the test area are shown as yellow circles in Figure 2.

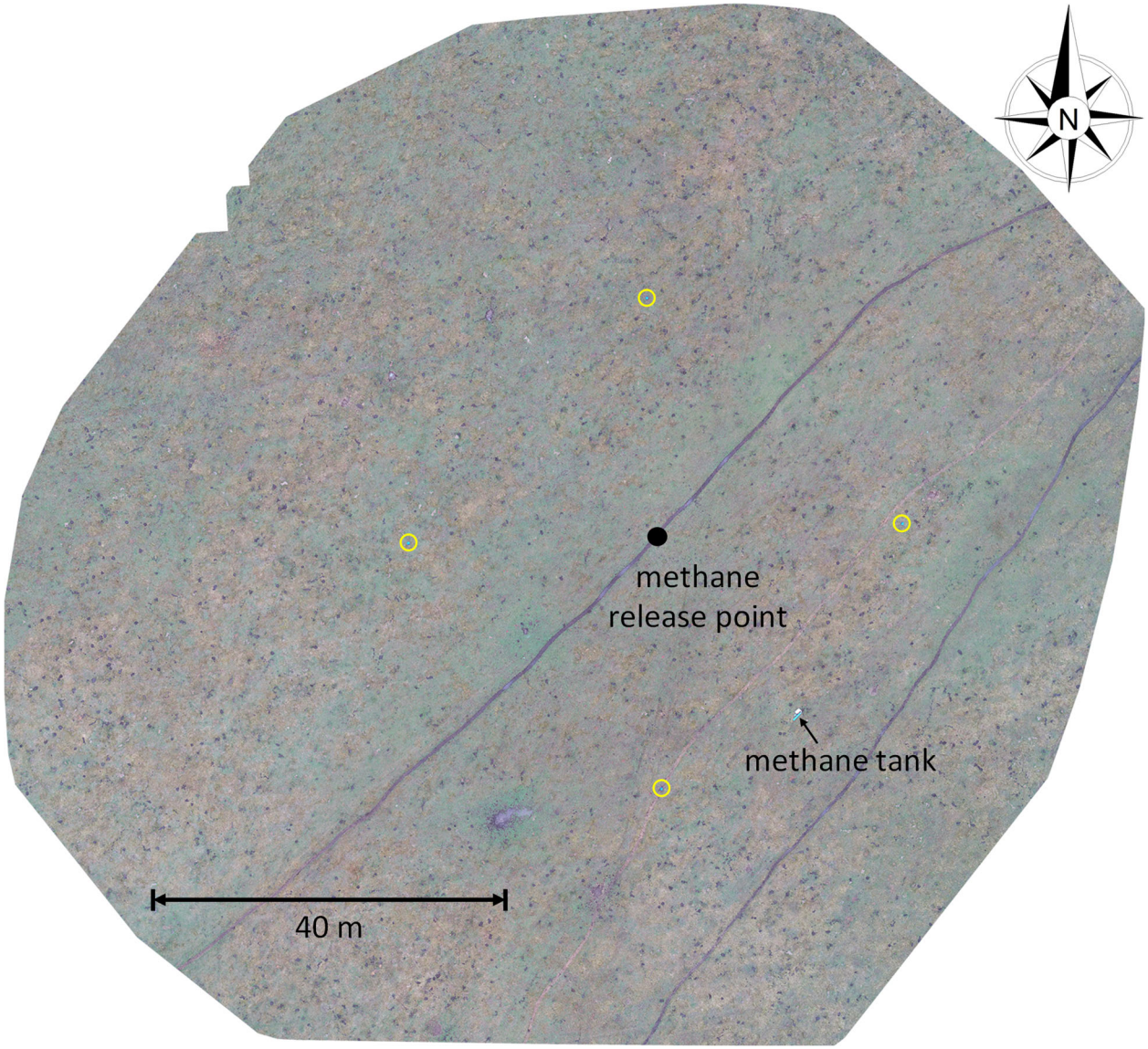

Figure 2. Orthophotograph of the test site in the open field.

The field was relatively flat and covered with a variable height of grass. The dark specks seen in Figure 2 are remnants of cow pats.

3.2 Weather Conditions

The wind and weather conditions at the time of the field experiments were assessed using data from the nearest weather station, visual observations, and data recorded by a nearby eddy covariance station.

The nearest Government of Canada weather station with hourly historical data is located at Fort St John, 70 km east of the test site. The weather conditions recorded at the Fort St John weather station are listed in Table 1.

Table 1. Weather data at Fort St John during the field experiments.

	Time	Temp. (°C)	Rel. Hum. (%)	Wind Dir. (10s deg)	Wind Spd. (km/h)	Stn. Press. (kPa)	Weather
August 29	10:00	15.3	62	24	11	92.33	Mostly Cloudy
	11:00	17.4	55	24	12	92.30	NA
	12:00	17.2	49	24	27	92.27	NA
	13:00	17.0	51	32	19	92.27	Mostly Cloudy
	14:00	10.8	89	31	18	92.38	Rain Showers
	15:00	11.8	89	31	17	92.38	Rain Showers
	16:00	12.9	82	28	18	92.39	Rain Showers
	17:00	12.0	83	25	25	92.42	NA
	18:00	11.5	84	27	19	92.44	NA
August 30	10:00	8.8	94	33	16	92.81	Cloudy
	11:00	9.0	87	32	22	92.86	NA
	12:00	10.6	73	32	21	92.90	NA
	13:00	10.7	73	31	21	92.95	Cloudy
	14:00	11.4	68	31	18	92.94	NA
	15:00	13.6	57	31	18	92.93	NA
	16:00	14.0	52	29	18	92.89	Mostly Cloudy
	17:00	12.7	61	20	8	92.88	NA

On August 29 between 13:00 and 17:30 at Fort St John when all the ground measurements occurred, the wind was coming from 250° to 320° at a velocity of 17 to 25 km/h. The sky was cloudy with rain showers. The temperature was between 12° and 17° C, and the barometric pressure was slowly rising.

On August 30 between 13:00 and 16:00 at Fort St John when all the drone flights occurred the wind was coming from 290° to 310° at a velocity of 18 to 21 km/h. The sky was cloudy. The temperature was between 10° and 14° C, and the barometric pressure was slowly falling.

Estimates of the wind velocity at the test site were obtained by applying the observational Beaufort wind velocity scale[1]. On August 29, a strong breeze equivalent to a speed of 10.8 to 13.8 m/s was observed at the test site. The prevailing wind direction was coming from approximately 315° based on a visual observation of a ribbon blowing in the wind. Rain showers were observed between 14:00 and 17:00 in the field that is consistent with the weather data in Table 1. On August 30, a light to gentle breeze (equivalent to a wind speed of 1.6 to 5.5 m/s) was observed at the test site when the drone was flying. The wind direction was noted to be quite variable from approximately 315° to 045°. The weather from 13:00 to 16:00 was clear and sunny.

The wind direction and velocity measured by an eddy covariance station set up at the nearby subsurface injection site are plotted in Figure 3 and Figure 4 for August 29 and 30, respectively. On August 29, at the beginning of the test period, the wind direction was coming from 345° to 360°, then changed to 030° at 16:00, and then shifted to approximately 180°. The wind speed first decreased from 0.7 m/s at 13:00 to 0.2 m/s at 16:00, and then increased to 2.2 m/s at 17:30. On August 30, the wind direction changed from 300° to about 180°, and then back to 300° during the testing phase. The wind speed increased gradually from 0.2 m/s at 13:30 pm to 0.8 m/s at 15:30 pm.

The difference in the observed and measured wind velocities may be related to how these are obtained. Visual observations are bias towards the peaks in the velocity, as the wind gusts are more likely to be noted in the field. Each measured velocity from the eddy covariance station is based on an average of measurements at 0.1 s intervals over the preceding 0.5 hour. Both field observations and eddy covariance measurements indicate that the wind velocity was higher during the ground-based fieldwork on August 29 compared to the airborne fieldwork on August 30.

[1] https://www.canada.ca/en/environment-climate-change/services/general-marine-weather-information/understanding-forecasts/beaufort-wind-scale-table.html

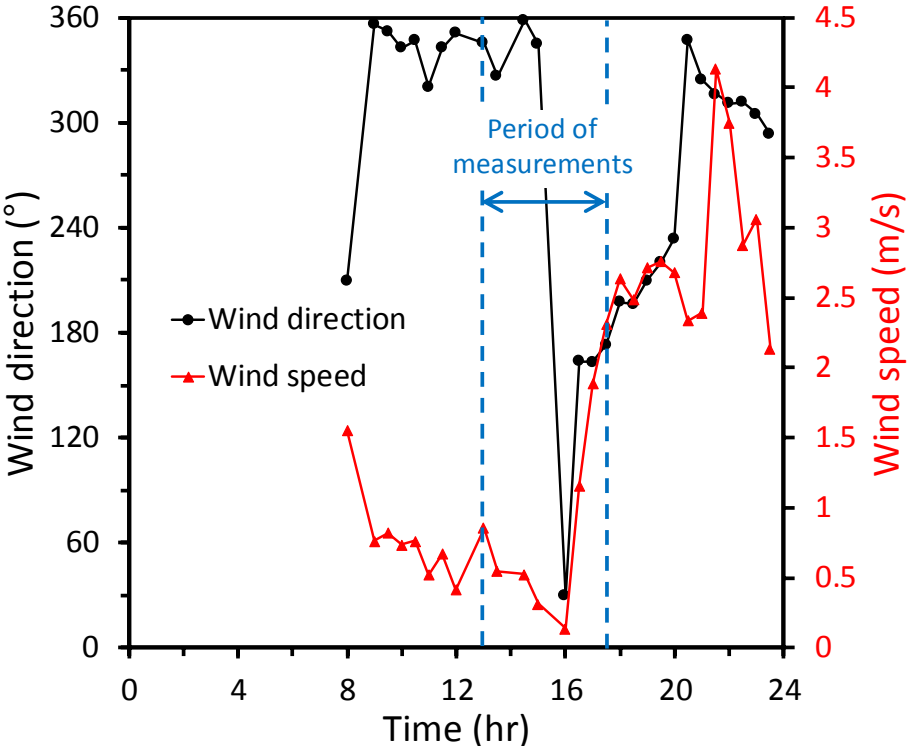

Figure 3. Wind direction and speed recorded by the eddy covariance station on August 29 (0.5 hr averages where data were available).

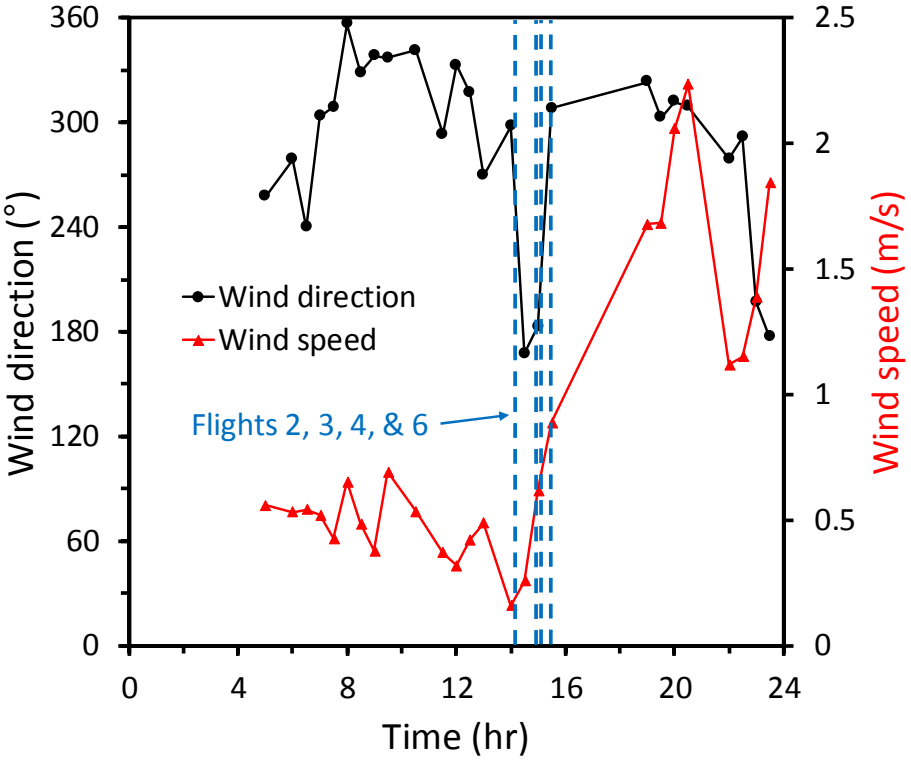

Figure 4. Wind direction and speed recorded by the eddy covariance station on August 30 (0.5 hr averages where data were available).

3.3 Ground Measurements

The measurement locations were set up in the open field by painting a grid pattern of reds dots on the ground at 5 m spacing. A surveyor's tripod, with the sensor, was set up at different locations along two perpendicular lines passing through the methane release point at the centre on the grid. A reflective target strapped to a surveying pole was successively moved from one dot location to another. Measurements were obtained by shooting laser beams from the methane sensor horizontally to the reflective target. Measurements of methane concentrations were taken at a frequency of 10 Hz and typically lasted for more than 30 s at each location to measure the temporal changes in methane concentrations.

The grid pattern of measurement points is shown in Figure 5. The four corners of the 40 m square are C1, C2, C3, and C4. The locations of the tripod with the methane sensor are T1 to T8. The methane sensor measured the methane concentration between the tripod location and a reflective target that was set up at different locations along the grid shown as red dots (typically 5 m apart) in Figure 5. Four target locations were placed 1 m from the centre of the square to obtain measurements near the release point (P1 to P4).

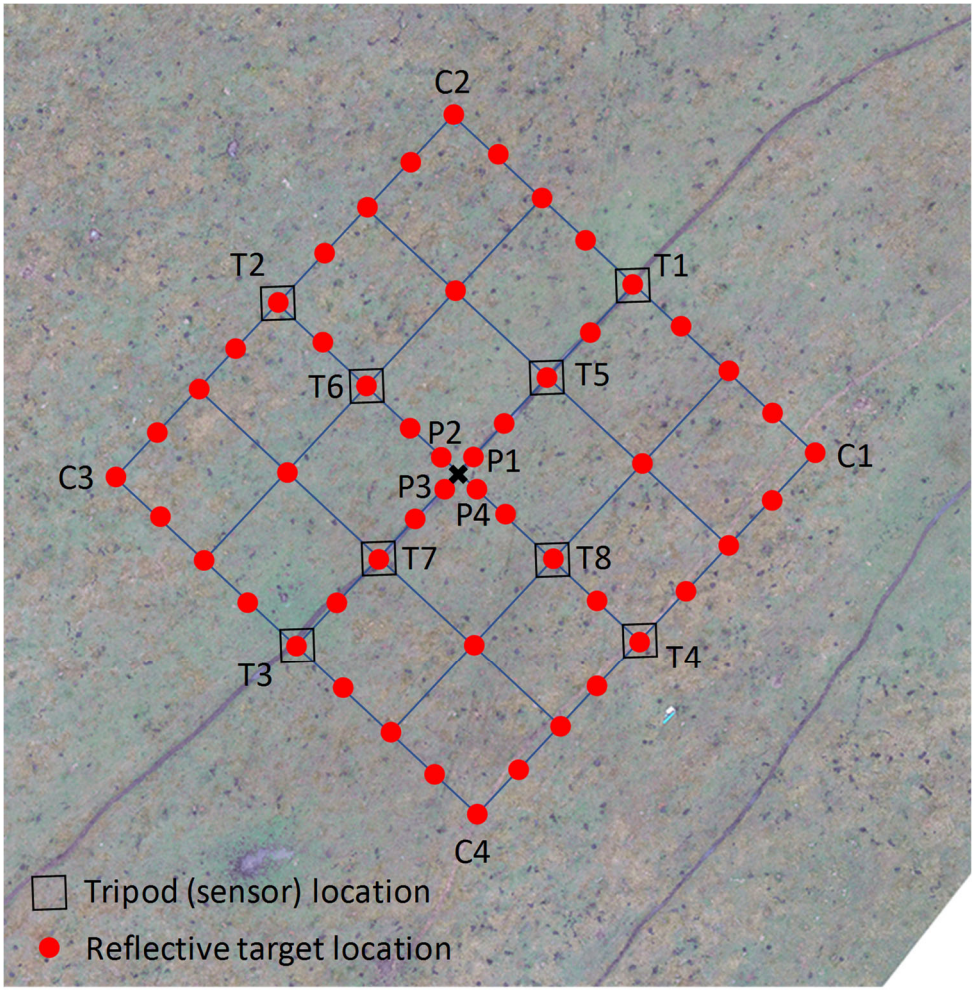

Figure 5. Layout of the ground-based measurement grid in the open field.

For the first series of tests, the gas line was set to release the methane at the ground level at a rate of 3 m^3/day. The sensor was set to measure methane approximately 1 m above the ground. Methane concentrations higher than the background level could not be detected, even when the methane release rate was increased to 30 m^3/day. There was a strong breeze in the field that quickly blew the methane laterally before it could vertically rise 1 m to the elevation of the methane sensor's laser beam. It was found that the methane gas release point should be at approximately the same height as the methane sensor's laser beam to allow for detection of higher methane concentrations. For the subsequent series of tests, the methane gas was released at 1 m above the ground, and the rate was set to 30 m^3/day.

3.4 Aerial Measurements

Measurements of methane concentrations were taken at a frequency of 10 Hz, giving a typical distance between measurements of 0.3 m when flying at a pre-programmed velocity of approximately 3 m/s. The drone was set to fly at 10 m height above the takeoff point, as this was recommended in the results of the previous report (Tannant et al., 2018). Flying in grid pattern was a viable option for this site because of the wide-open space and reduced risk of the drone running into trees. Flight times ranged between 2 and 5 minutes, mostly due to an unexpectedly short battery life of the drone.

For all drone flights, the methane gas was released at 1 m above the ground. The methane gas release rate was varied from 10 to 30 m^3/day for different flights to investigate the influence of the release rate on the methane measurements.

3.5 Challenges

There were a few challenges encountered in the field when performing ground-based measurements. The methane sensor was not able to pick up methane measurements higher than the background concentration when the methane sensor's laser beam was located 1 m higher than the gas release point. A likely explanation is that the wind blew the methane laterally before the methane elevated to a higher elevation. High methane concentrations were recorded when the methane sensor's laser beam was lowered to the same elevation as the methane release point. One implication from this finding is that when using a laser-based methane sensor for detecting methane leakage, it is important to shoot the laser beam directly into the suspected source area of leakage, especially on windy days. It may also be helpful to stand down-wind of the source area (if safe to do so) and shoot the laser beam upwind to the suspected source area to increase the chance of detecting higher than background levels of methane.

The methane sensor shoots a green laser beam to assist in identifying where the methane detection beam will travel. However, it is difficult to align or see the green dot on a reflective surface that is further than 15 to 20 m away from the sensor.

There were some difficulties getting the GasViewer software on the phone to establish a Bluetooth connection with the methane sensor so that the devices would communicate with each other. Usually restarting the software resolved this issue.

There were several issues in the field with the drone not being able to establish its location due to poor communication with the GPS signal and other software issues. Drone flights were planned with flight control software installed in a laptop and were executed with an app installed in a tablet, and neither had a built-in GPS. There was no direct way to associate locations in the field with positions on the map in the laptop and tablet. Physically walking the drone with a built-in GPS to the corners of the desired flight boundary was attempted to obtain the corresponding GPS coordinates. However, attempts to input the obtained GPS coordinates into the flight control software for the desired flight boundary was not successful. Trial and error had to be performed in the field to fly the drone approximately within the desired flight boundary.

The originally planned flight grids had to be flown with a wider spacing between rows because of limited available flight time due to reduced battery life (old batteries) and a missing charger. During some flight attempts, the drone landed automatically due to low battery warnings. Of the seven flights that were attempted, only three were fully completed. The release of methane was stopped between flights.

The lesson learned here is that even though we used a survey company with years of experience flying drones, the drone technology has improved and the company is losing experience and expertise in flying larger drones as they shift their routine fieldwork to smaller UAVs such as the DJI Phantom 4 Pro. A large drone was needed to carry the methane detector and smart phone, but the drone batteries were getting old, and the flight control software that was specific to this drone is not routinely in use by the company. These factors contributed to limitations and challenges in performing the fieldwork. Performing airborne surveys with the Laser Methane mini-G is far more difficult than doing ground-based measurements and requires an appropriate drone, flight controller software, and experienced personnel. In practice, these could only be reliably be performed by a company or crew that routinely does this type of work.

4 Results

4.1 Data Processing

Processing of the raw recorded data was required to obtain meaningful data of methane concentrations at specific locations. The methane concentration data recorded by the methane sensor along with its GPS locations recorded by the phone are saved as a CSV file. Methane concentration, intensity, and error code are recorded every 0.1 seconds while the GPS locations from the phone are recorded every 0.5 seconds. There were error codes associated with some methane measurements. Measurement data with error codes were not used.

For the aerial surveys, the GPS locations and the heights for a flight recorded by the drone are saved as a separate CSV file. The GPS locations, altitude above takeoff, and time were recorded every 0.5 seconds during the flights. It was found that the GPS locations recorded by the phone have low accuracy based on last year's field test (Tannant et al., 2018) thus they are not used in the following analysis. Instead, the GPS locations recorded by the drone, which have higher accuracy, are used as the locations to analyze and plot methane measurements. By matching the time stamps that were recorded in both CSV files, a methane concentration corresponding to the drone at a specific GPS location and a height from the ground can be determined.

The LMm-G sensor records methane concentration in ppm·m observed in a column of air. Therefore the higher the drone is flying or the further the sensors was away from a reflective surface on the ground, the larger these measurements will be given a uniform concentration of methane in the air. The average methane concentrations were calculated as the measured methane concentration divided by either the height of the drone above the ground or the distance from the reflective surface to obtain ppm values.

Before plotting the concentration data, the points were further filtered by eliminating concentration measurements observed at a drone height of lower than 8 m above the takeoff point. These are associated with the takeoff and landing locations of the drone.

The collected data can be transferred into Geographic Information System (GIS) software programs for display purposes. For example, Google Earth can be used to display the points as a KML file, or they can be added as a Shapefile layer overlying an orthophotograph in ArcMap. The user can easily identify areas of high methane concentration referenced by their GPS coordinates, or relative to natural landmarks on the orthophoto. For the airborne data, smartphone GPS coordinates were not used to display the flight paths and concentration data. Instead, the more accurate GPS coordinates recorded by the drone were used.

A schematic of the data processing procedure used for the airborne data is shown in Figure 6.

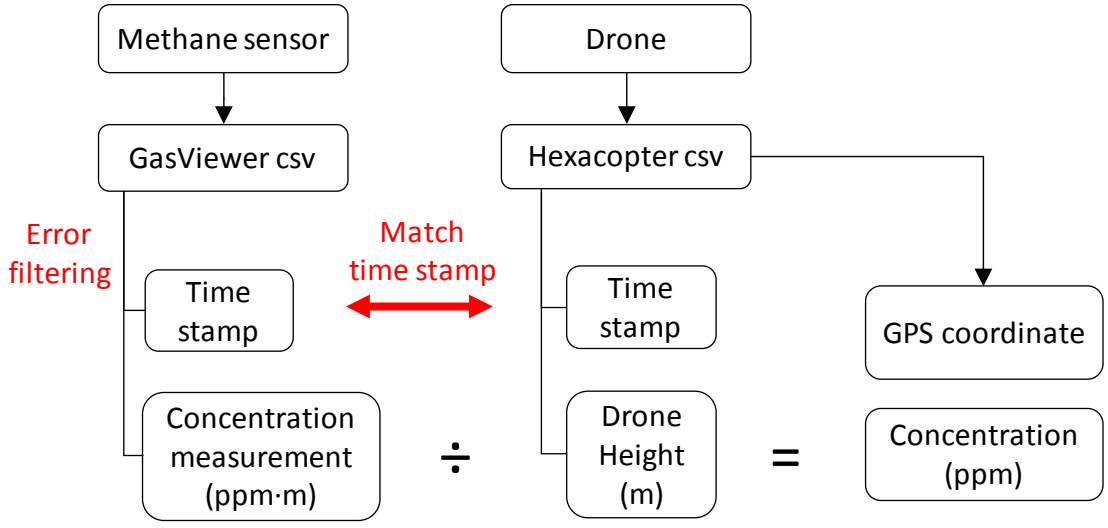

Figure 6. Data processing procedure.

4.2 Ground-Based Measurements

On August 29, 2018, a series of ground-based measurements to map controlled surface release of methane was conducted over 4.5 hours within the open field. A summary of ground measurement data is listed in Table 2. The data from a series of attempts to measure the methane when the release point for the gas was at ground level are not presented. Two sets of measurements were discarded for the set-up at T4 because there was confusion as to the locations of the reflective target when the measurements were taken.

Table 2. August 29 ground measurement data.

Station	Start time (hh:mm:ss)	Duration (mm:ss)	Methane release rate (m^3/day)	Comment
T1	13:21:32	03:36	0	T1→C1
T1	13:25:31	02:27	0	T1→Centre
T1	13:28:22	02:33	0	T1→C2
T1	15:21:04	10:32	30	
T2	15:35:23	11:20	30	
T3	15:51:35	11:37	30	
T4	16:15:12	15:05	30	
T5	16:56:19	06:08	30	
T6	17:05:31	03:09	30	
T7	17:11:45	04:29	30	
T8	17:18:49	13:04	30	

Before the methane was released, measurements were taken from T1 in three directions to measure the background methane concentrations. The prevailing wind near the ground surface was roughly coming from the northwest to north based on visual observations of a ribbon blowing in the field. The results of methane measurements are plotted in Figure 7. The background concentration fluctuates mostly from 2 to 2.5 ppm. The average background methane concentrations are 2.2, 2.3, and 2.1 ppm along directions of T1→C1, T1→C, and T1→C2, respectively.

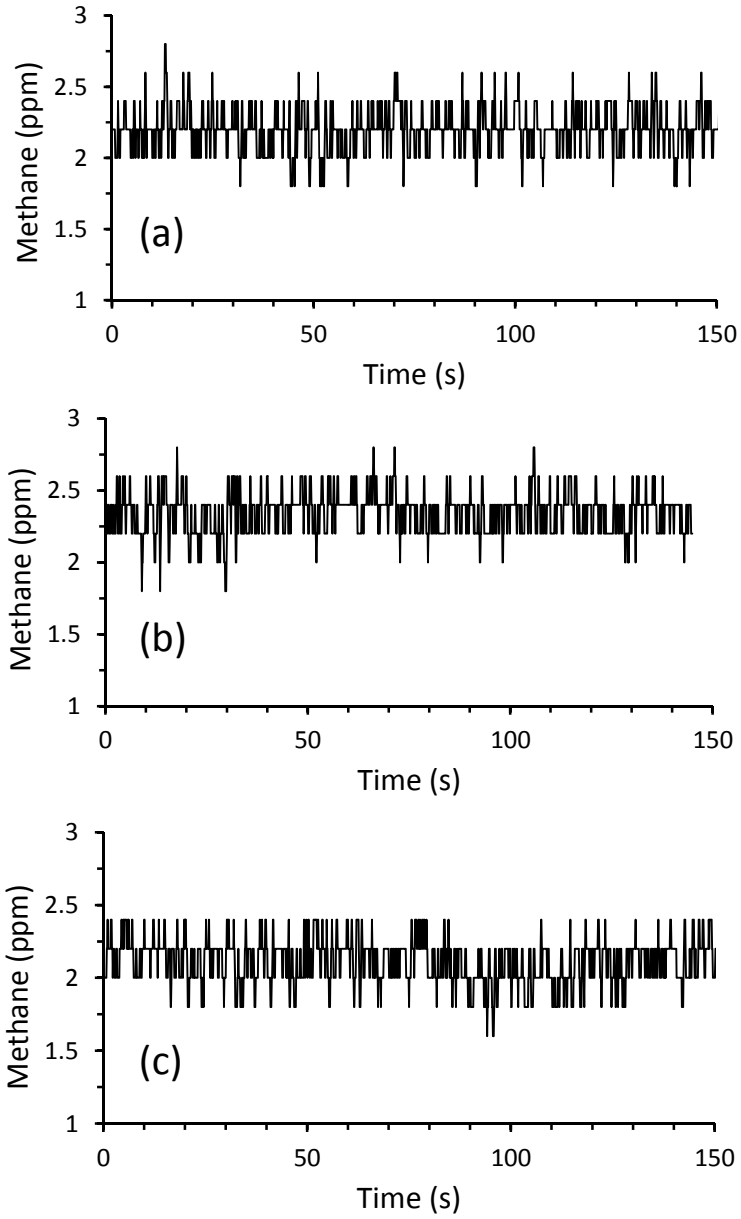

Figure 7. Background methane concentration along (a) T1→C1, (b) T1→Centre, and (c) T1→C2.

Figures 8-11 show the results from measuring the methane concentrations for selected locations around a release point that was 1 m above the ground. Note that the prevailing wind direction during these measurements shifted significantly over the 2 hr period of measurements from the north to the south (Figure 3). As seen in Figure 8, for measurements conducted in areas that are upwind relative to the release point, the methane concentration is close to the background concentration (T1→C1, T1→C2, and T1→P1). When measuring from T1 to P3, only one spike indicating high methane concentration was mapped during a 50 s measuring period. When measuring from T2 to P2 and P4, much higher methane measurements were found as shown in Figure 9. The reflector station P4, which was downwind of P2, yielded much higher methane concentration. When measuring from T3, the laser path

T3→P3 recorded a concentration similar to the background methane concentration. The laser path T3→P1 gave some high spikes (Figure 10) because the laser beam happened to pass through the methane release point. Laser paths T4→P4 and T4→P2 had higher methane concentrations than the background level (Figure 11). The concentration of T4→P4 is lower than T4→P2 as expected.

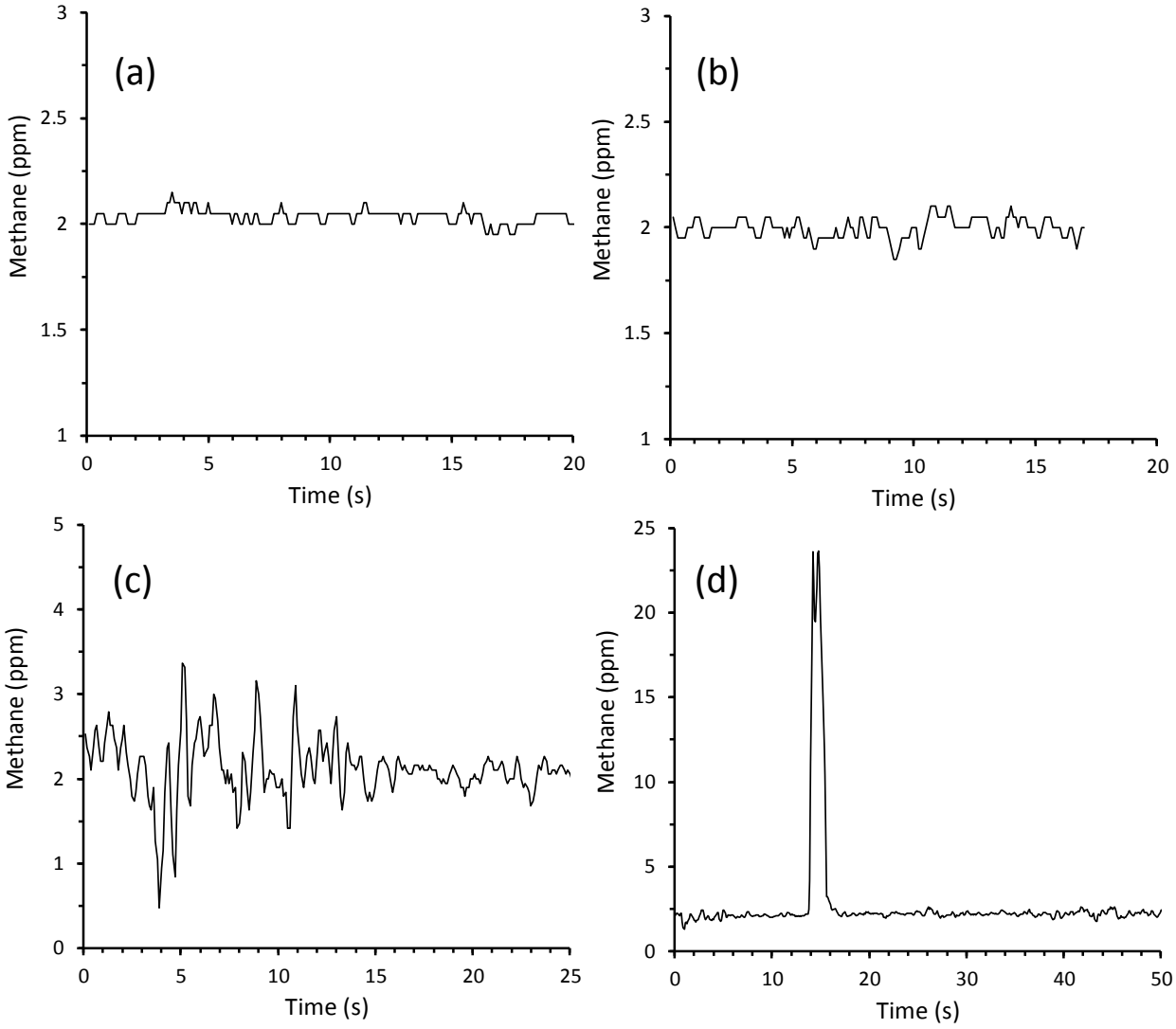

Figure 8. Methane concentration measured for laser beam paths (a) T1→C1, (b) T1→C2, (c) T1→P1, and (d) T1→P3.

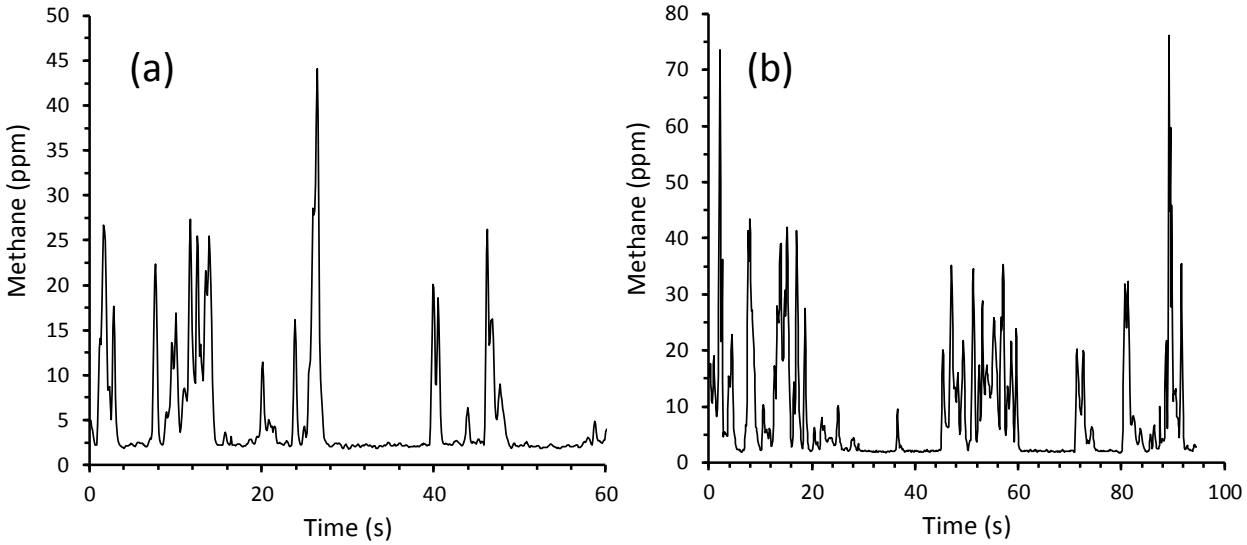

Figure 9. Methane concentration measured for laser beam paths (a) T2→P2, and (b) T2→P4.

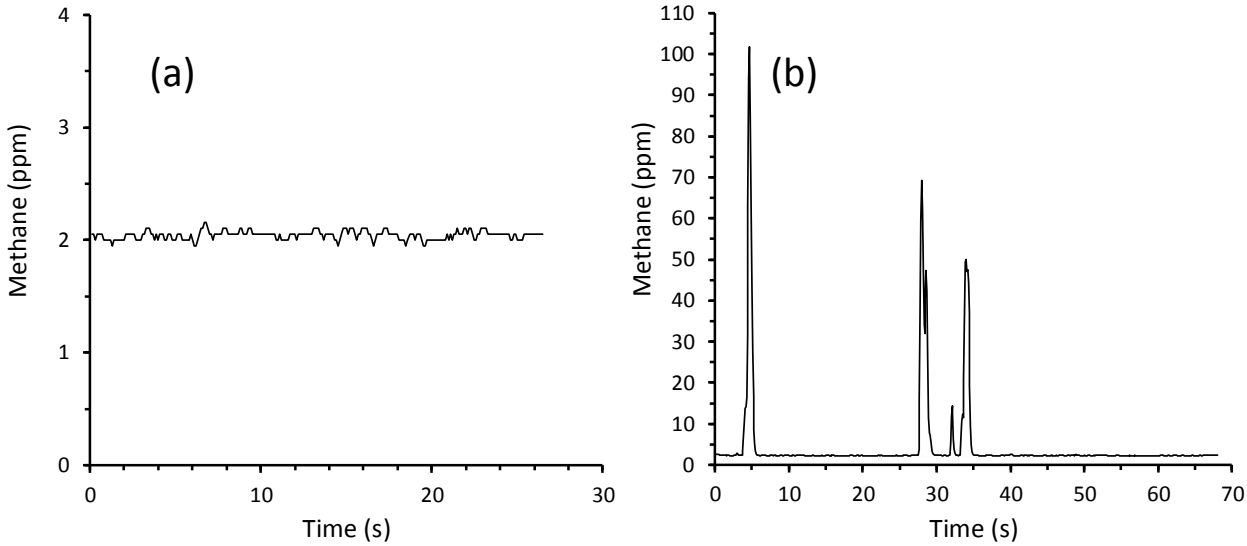

Figure 10. Methane concentration measured for laser beam paths (a) T3→P3, and (b) T3→P1.

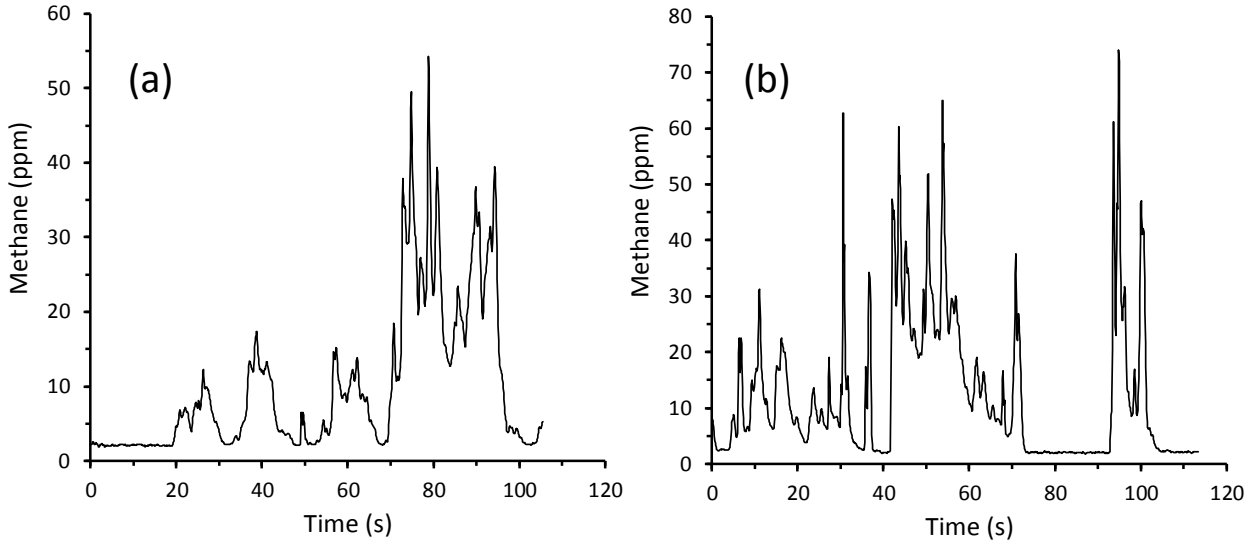

Figure 11. Methane concentration measured for laser beam paths (a) T4→P4, and (b) T4→P2.

It can be seen that wind direction greatly changes the distribution of the released methane and higher methane concentrations are found in areas that are downwind of the gas release point. Furthermore, the methane concentrations quickly change over time in response to changing wind direction and velocity. Interestingly, the methane concentration did not remain at an elevated uniform value for any of the measurements. Instead, where methane concentrations above the background level were detected, the concentrations shows multiple spikes separated by short periods of time when the methane concentration fell to background levels. For the breezy field conditions and the point source of methane located 1 m above the ground, there is no indication that a uniform plume of methane was generated in the atmosphere.

To obtain an overall indication of the distribution of methane around the methane release point, the average value and the standard deviation of methane concentrations over the measuring period were calculated for each location. Note that the average value and the standard deviation were plotted at a point located mid-way between the sensor and reflector locations. For example, if the measurement was obtained from T1 pointing to a target 5 m away, the average concentration for this 5 m laser path length is plotted 2.5 m away from T1. Measurements were performed at different locations by moving the reflective target along the grid lines in 5 m increments (except for locations P1 to P4, which were 1 m away from the release point). The average methane concentration over, for example, a 5 m segment was determined by subtracting the methane reading in ppm·m by the value measured at a previous location, which subsequently was divided by the length of the segment to get the average value in ppm. For example, assuming the reading of the methane sensor is 10 ppm·m when the target is 5 m away, and the reading is 30 ppm·m when the target is 10 m away. Then the average concentration over a segment that is 0-5 m away from the sensor is 10 ppm·m /5 m = 2 ppm, and that over a segment that is 5-10 m away from the sensor is (30 ppm·m – 10 ppm·m)/(10 m - 5 m) = 4 ppm.

The average value and the standard deviation of methane concentrations are shown in Figure 12. 3D views of methane distributions were plotted using the "surf" function in MATLAB. As expected, much higher average methane concentrations were mapped near the release point, and areas that were downwind had higher concentrations than areas that were upwind relative to the release point. Also, higher standard deviations of methane concentrations were mapped near the release point and the areas that were downwind relative to the release point, indicating that their methane concentrations changed over the measuring period.

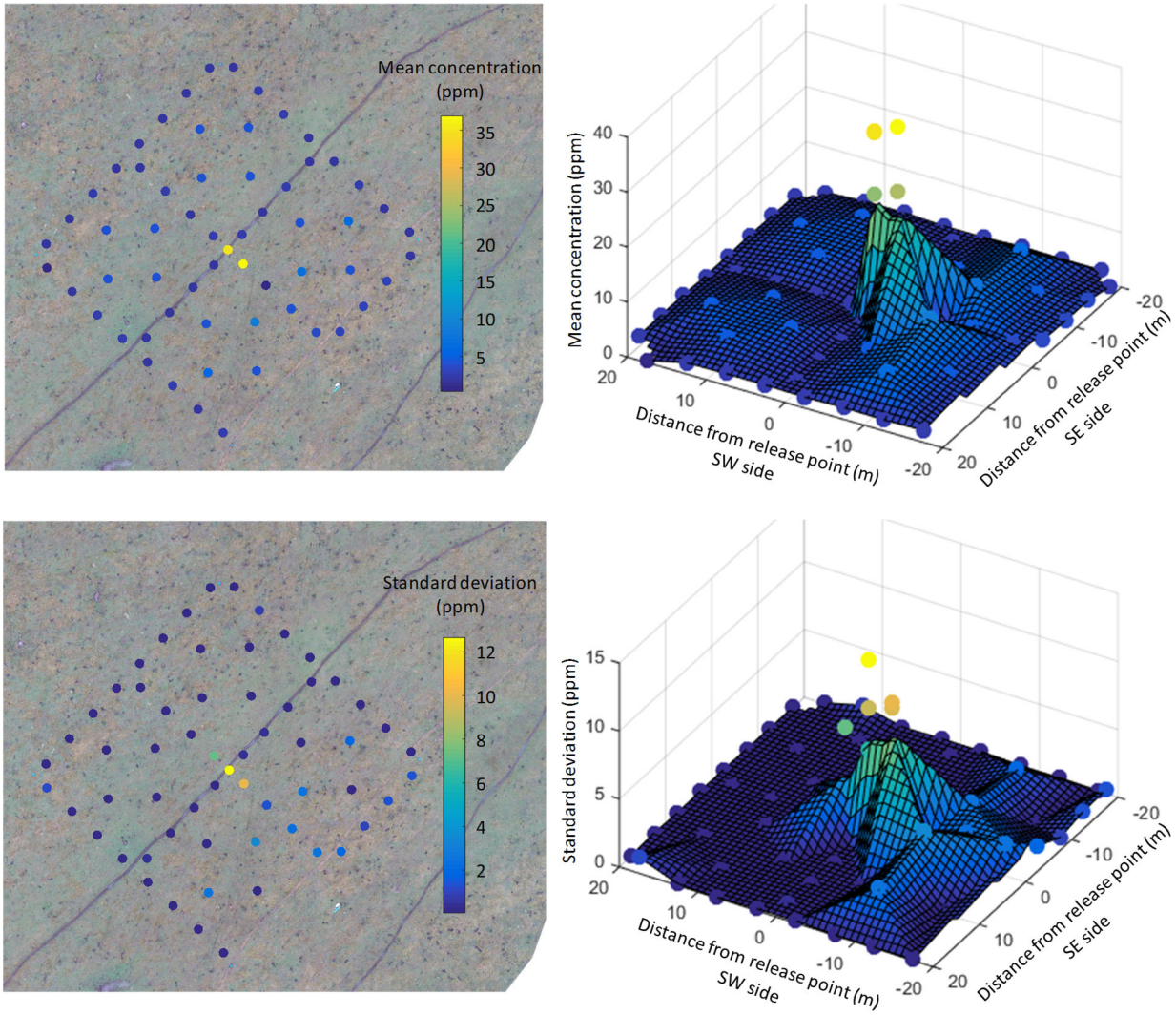

Figure 12. Plan and 3D view of mean and standard deviation of methane concentrations near the release point.

4.3 Drone-Based Measurements

The flights that were flown on August 30, 2018, were approximately 10 m above the takeoff point. Figure 13 is a photo of the drone flying over the open field. Seven flights were attempted, but not all were successfully completed. Detailed information for the flights is

shown in Table 3. A total of 888 litres of compressed natural gas (at standard temperature and pressure) were released during this testing phase.

Figure 13. Drone flying over the open field during a surface-controlled release.

Table 3. August 30 flight data.

Flight	Start time (hh:mm:ss)	Duration (mm:ss)	Methane release rate (m^3/day)	Comment
1	13:29:06	02:17	20	flight terminated early
2	14:11:13	04:29	20	
3	14:52:40	02:04	10	Partial coverage
4	15:00:59	05:21	10	
5	15:14:31	01:32	30	flight terminated early
6	15:23:43	04:45	30	
7	15:36:45	01:06	20	flight terminated early

The flight paths of the seven drone flights are plotted on the orthophoto of the open field as shown in Figure 14. Flights 1, 5, and 7 were aborted in the middle of flights due to battery voltage shortage and other technical issues. Flight 3 only covered a portion of the desired area due to difficulties in identifying the flying boundary when designing the flight path. Flights 2, 4, and 6 provided the most useful data.

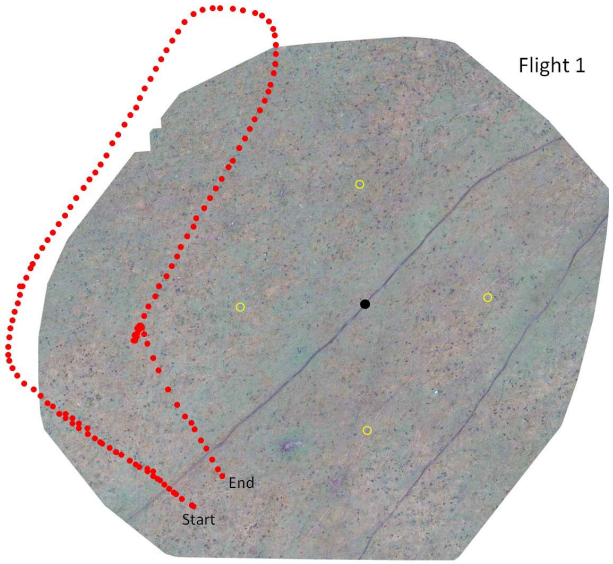
Flight 1
End
Start

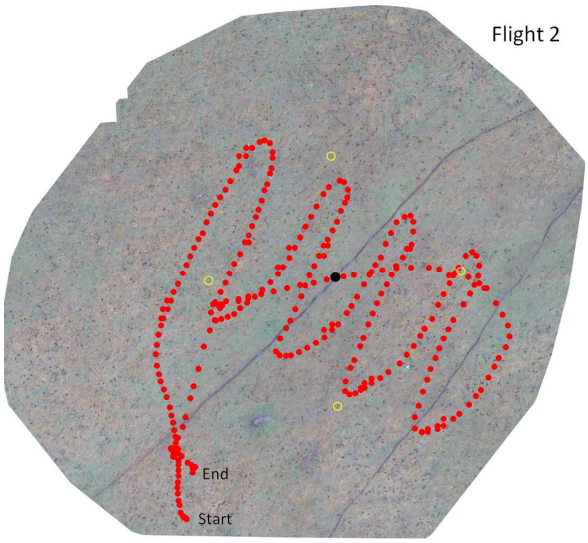
Flight 2
End
Start

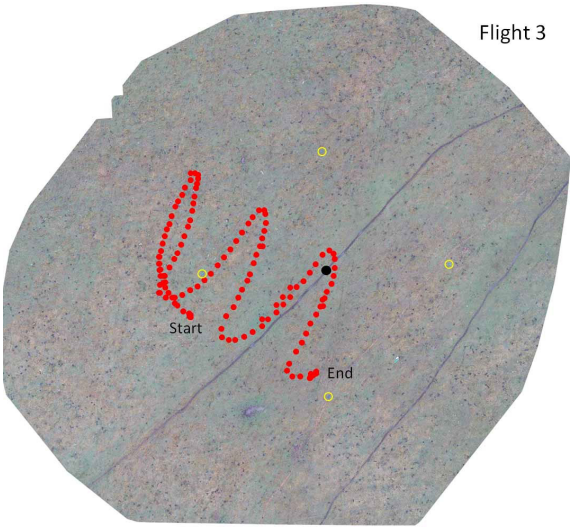
Flight 3
Start
End

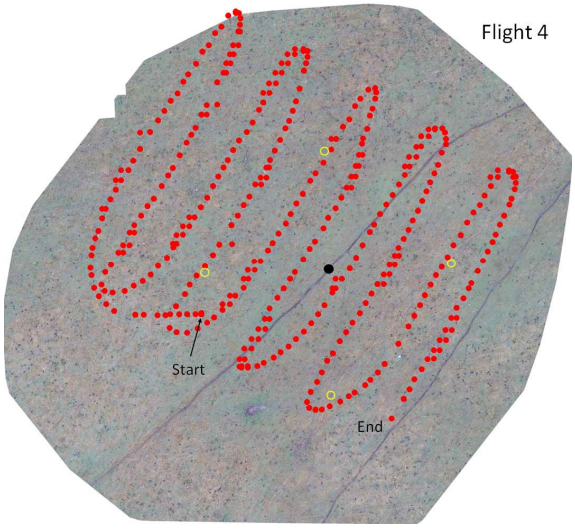
Flight 4
Start
End

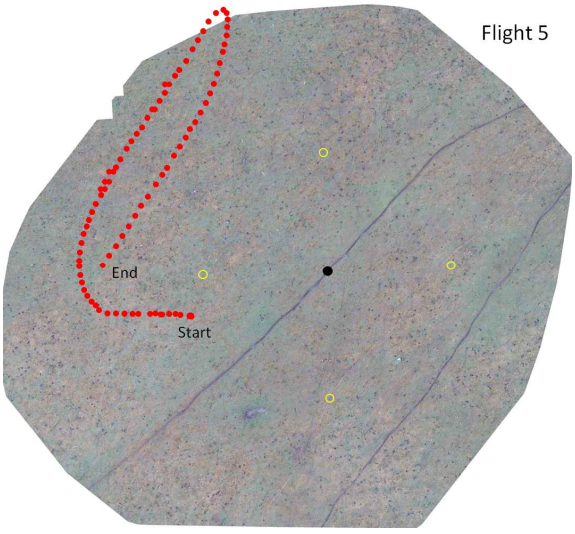
Flight 5
End
Start

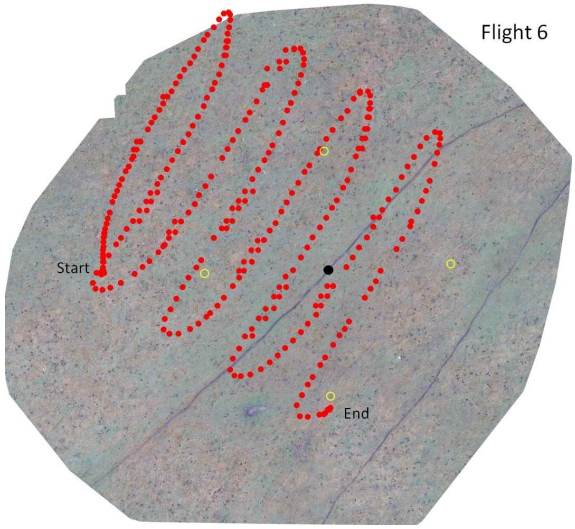
Flight 6
Start
End

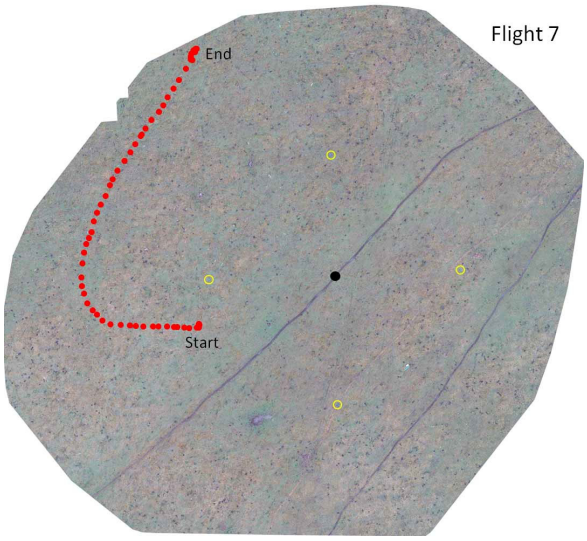

Figure 14. Paths flown by drone for seven flights.

The methane concentration measurements obtained from the drone flights are summarized in Table 4. The methane concentration data (after data processing as outlined in Section 4.1) from flights 2, 3, 4, and 6 are plotted over the orthophoto of the open field in Figure 15 to Figure 18. Data measured during flight takeoff and landing are not included in the plots. Flights 1, 5, and 7 with limited data are not plotted.

Table 4. Summary of methane concentration measurements.

Flight	Comments
1	Only a few measurements near the takeoff location were valid; these ranged from 0.5 to 8 ppm.
2	The drone was flown over the release point, and the methane concentration ranged from 0 to 5.5 ppm. Most of the area covered by the flight had a methane concentration close to the background concentration.
3	Most of the locations mapped were west of the release point, and a few high methane concentrations from 5 to 8.5 ppm were measured.
4	Measured methane concentrations ranged from 0 to 6.5 ppm. Most of the high concentrations were located W to NW of the release point.
5	A few available valid measurements have a concentration from 1 to 3 ppm, which was close to background methane level.
6	Measured methane concentrations higher than 5 ppm occurred S and NW of the release point, while most of the measurements were less than 4 ppm
7	Several locations NW of the release point had a concentration higher than 30 ppm.

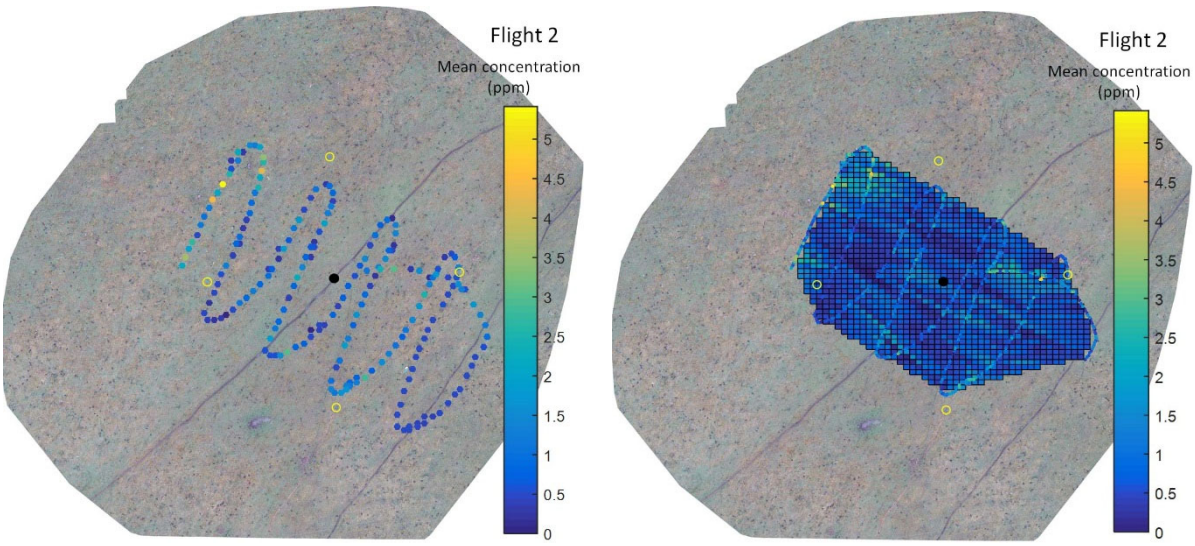

Figure 15. Valid methane concentration measurements and methane distributions for flight 2.

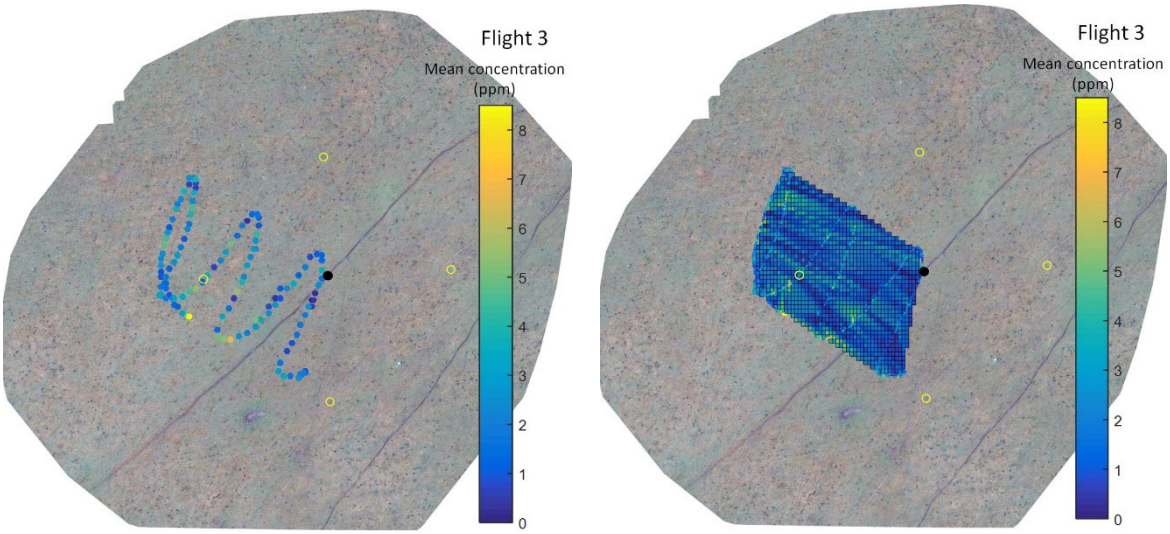

Figure 16. Valid methane concentration measurements and methane distributions for flight 3.

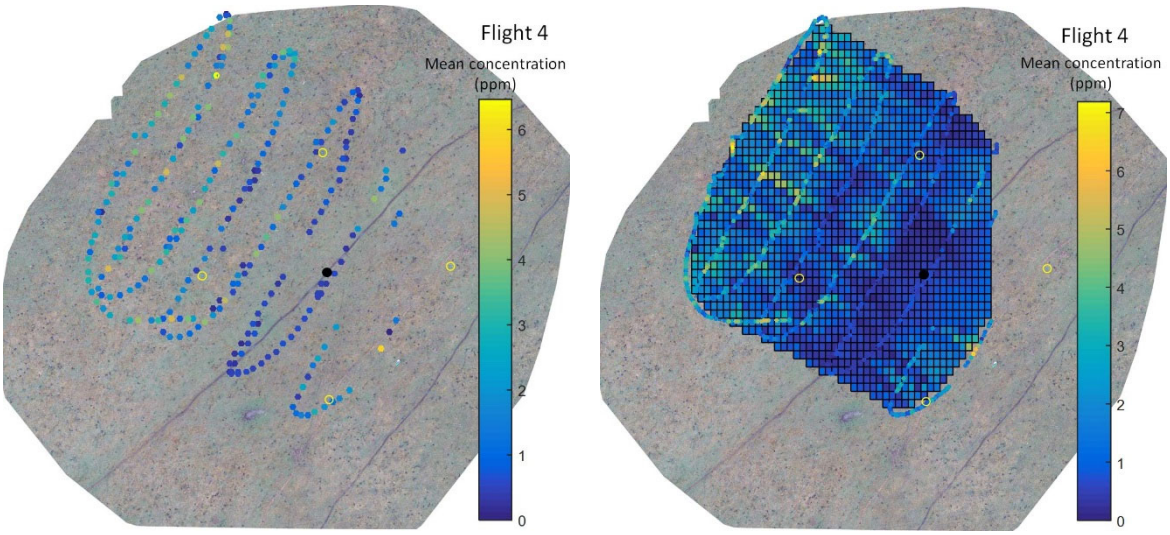

Figure 17. Valid methane concentration measurements and methane distributions for flight 4.

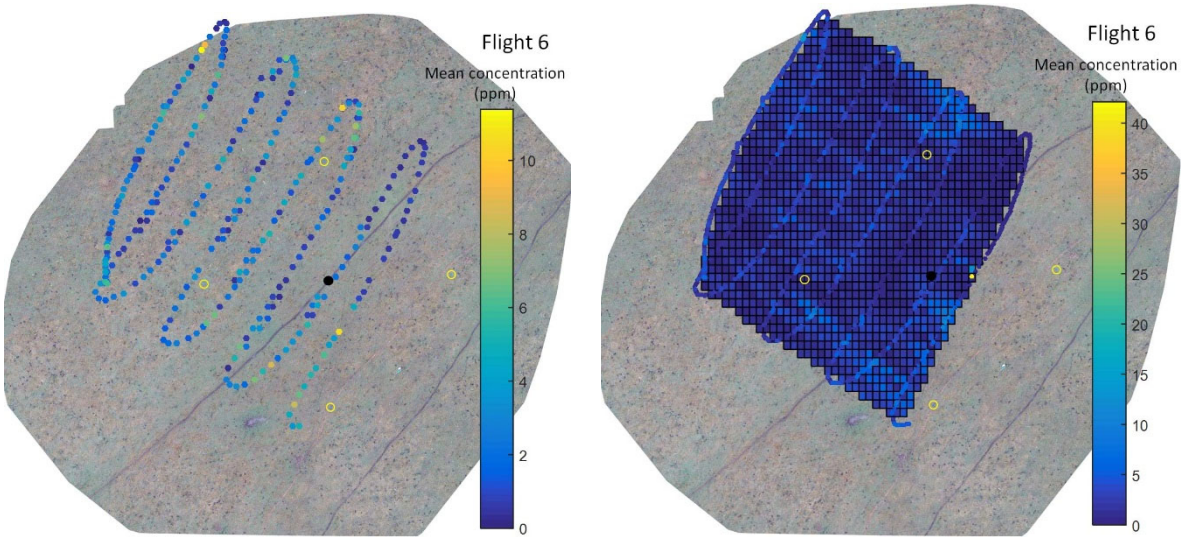

Figure 18. Valid methane concentration measurements and methane distributions for flight 6.

Due to a difference in measurement frequency, there are more methane sensor measurements than GPS locations. The methane measurement data recorded between times of GPS measurements were plotted between GPS locations assuming that the drone flew at a constant velocity between two adjacent GPS locations. The data plotted in Figure 15 to Figure 18 were used as the input to the 'surf' function in MATLAB to create methane distribution maps, which are shown in the same figures. No obvious methane plumes were mapped.

5 Discussion and Conclusions

The fieldwork conducted in 2018 provided an opportunity to evaluate the use of a drone and a laser-based methane sensor for measuring methane concentration around a metered point

source for the release of methane into the air. This work was an extension to the fieldwork that was performed in 2017 and reported by Tannant et al. (2018).

Seven drone flights were attempted at a 10 m elevation above the ground surface, and more than 13,000 methane measurements were obtained, of which more than 85% were valid data. The fieldwork in 2018 encountered a few challenges. Three flights had to be aborted in the middle of the flight due to low drone battery life. The flight control software combined with limited flight crew experience with a larger drone that is now rarely used did not provide the desired grid-pattern centred over the methane release point.

The methane sensor was able to measure background or ambient methane concentrations in the air. At the test site, this value was roughly 2.2 ppm, although it ranged between 0.5 and 3 ppm. Thus, when the measured values exceeded roughly 3 ppm, this was evidence that some of the released methane was being detected. Methane concentrations above 10 ppm were observed both by ground-based and drone-based measurements during the testing.

The fieldwork indicated that the methane plume originating from a surface point source varied quickly in space and time, probably largely in response to changes in the wind velocity and direction, including wind turbulence near the ground surface. Ground-based measurements at the same elevation as the release point recorded high concentrations (>35 ppm) near the release point when the methane was released at a rate of 30 m^3/day. Methane concentrations greater than 5 ppm were recorded in areas that were within 15 m of the release point in the downwind direction. For drone-based measurements, most concentration measurements were under 10 ppm, except for a few locations with concentrations as high as 60 ppm. Areas with high concentrations tended to be isolated points around the methane release point and were generally downwind of the release point.

The maximum practical height for using a Laser Methane mini-G sensor when flying over grassy terrain or low vegetation is approximately 10 m above the ground. If flying over a well pad without vegetation, a slightly higher altitude would probably also work.

Because a relatively large and complicated drone is needed to carry the Laser Methane mini-G, this greatly increases the complexity for conducting airborne measurements versus ground-based measurements. This implies the need for a highly trained crew to perform the field measurements. However, the key components in the Laser Methane mini-G could be reconfigured into a much lighter instrument, without the need for a smart phone, which could greatly simplify the fieldwork. If a laser-based sensor could be constructed that was light enough to be carried by a smaller drone, such as a DJI Phantom 4, then the drone-based measurement option becomes much more feasible. Given that very few Laser Methane mini-G instruments are in routine use, it is unlikely that there is currently enough demand for a company to design and make a lightweight version of this sensor.

References

Cahill, A.G., Chao, J., Ford, O., Ladd, B., Prystupa, E., Mayer, K.U., Tannant, D., Black, A., Crowe, S., Hallam, S., Mayer, B., van Geloven, C., Welch, L., Levson, V. & Beckie, R.D. 2018. Establishment of field stations for the multidisciplinary study of controlled natural gas releases, northeastern British Columbia. In Geoscience BC Summary of Activities 2017, Geoscience BC, Report 2018-1.

EERI. 2018. Hudson's Hope field research station - controlled natural gas release investigations. Energy and Environment Research Initiative. http://eeri.ubc.ca/current-research-projects/hudsons-hope-field-research-station/

Tannant, D., Smith, K., Cahill, A., Hawthorne, I., Ford, O., Black, A., and Beckie, R. (2018). Evaluation of a Drone and Laser-Based Methane Sensor for Detection of Fugitive Methane Emissions. Submitted to the British Columbia Oil and Gas Research and Innovation Society, February 1, 2018.